

OPTICAL MICROSCOPY CHARACTERISATION OF FUSION LINES OBTAINED ON AUSTEMPERED DUCTILE IRON BY LASER BEAM WELDING WITHOUT PREHEATING

I.C. MON¹ M.H. TIEREAN¹ L.S. BALTES¹

Abstract: *This study concerned the weldability of austempered ductile iron using laser welding. Was explored the operational window power - welding speed making the fusion lines on plates without preheating using as criteria the absence of the welding defects and the geometry of the fusion lines. The laser welds were characterised by optical microscopy on fusion lines, heat affected zone and melted zone. The results show the applicability of this laser beam welding technology to reduce and even eliminate the cracking phenomenon.*

Key words: *Austempered Ductile Iron, laser, welding, microscopy.*

1. Introduction

Austempered Ductile Iron (ADI) is a new engineering material with an exceptional combination of mechanical properties and important applications in various fields. Austempered Ductile Iron is obtained from spheroidal graphite iron (Ductile Iron - DI) after the heat treatment of austenitizing at 850...950 °C for 0.5...3.5 hours, followed by rapid quenching to the isothermal transformation temperature 235...450 °C, with 0.5...4 h maintenance [16]. The final microstructure of ADI includes: ferrite, pearlite, martensite and ausferrite [5].

This new material has received numerous names over time, finally at the world conference on these cast irons, at Indian Lake Resort, Chicago, USA, 1991, the name of ausferrite spheroidal graphite cast iron was agreed. The term used in English language (articles, books, internet) is Austempered Ductile Iron, abbreviated ADI [6].

In the late 1960s, General Motors began replacing the cogwheel and differential pinion from cars made of cemented steel with ADI. In 1977 General Motors began the production of ADI for gear sets of Pontiac engines, thus replacing the AISI 8620 steel. From 1970 to the present, the ADI market has experienced a rapid development, estimating that by 2020 it will reach a production of 500 000 tons per year [7]. The ADI can be

¹ Dept. of Materials Engineering and Welding, *Transilvania* University of Braşov, Romania.

welded after austenitization and isothermal transformation heat treatment or as in DI case, the heat treatment being performed at the end.

In [15] there are presented the main problems during welding of ADI: (i) the formation of carbides in the as-welded ductile iron as well as the partial fusion zone due to fast cooling rate leading to cracking and (ii) the properties of ADI weld should match those of ADI however the welding temperature would necessarily damage the structure of ADI.

Paper [11] presents a review on tests of austempered ductile iron welding. Researches on GTAW/SMAW weldability of ADI/DI were presented in [13] and researches on laser welding on ductile iron plates were presented in [12].

By applying the MMA welding process and using the Conarco Ni55 electrode (50% Fe and 50% Ni) ADI can be welded at room temperature of 22°C, obtaining low values for the mechanical properties of the welded joint compared to those of the base material ADI [1]. Attempts were made to repair ADI cast iron components from military vehicles using the WIG welding process. In the microstructure of the base material the presence of the upper ausferrite is highlighted, and in the welding zone the presence of ledeburite. The results obtained were applied to the lower arm axle of the military vehicles [10]. Intensive research has been performed to optimize the parameters of the laser welding regime [3, 4, 8] and improving material's properties [2, 9].

The goal of present research is the testing of laser beam weldability of austempered ductile iron without preheating, using optical microscopy. Next papers will contain the other characterizations.

2. Materials and Methods

The material used in the experimental research to perform laser beam welding tests without additive material was ADI, Grade 1050/750/07 (ASTM A897M-03), provided by the Central Metallurgical Research and Development Institute Egypt. The chemical composition of the ADI specimens is presented in Table 1 according to the specification received from the manufacturer [14].

Chemical composition of ADI samples (mass %)

Table 1

C	Si	Mn	P	S	Fe
3.5...3.6	2.4...2.5	0.25...0.3	0.01	0.01	balance

To perform the experimental tests on ADI, the specimens have been cut to the dimensions of L x W x H = 110 x 55 x 6 mm. The required minimum values of the mechanical properties of ADI are presented in Table 2.

Mechanical properties of ADI according to ASTM A897M-03 [17]

Table 2

Grade	Tensile strength [MPa]	Yield strength [MPa]	Elongation [%]	Impact energy [J]	Brinell Hardness [HB]
1050/750/7	1050	750	7	80	302-375

The fusion lines on ADI samples (Figure 1) was performed using Truedisk 6002 laser source at Bourgogne University, Laser and Materials Treatments laboratory, Le Creusot, France. The generated laser beam was in the infrared range characterized by a wavelength of 1.06 μm and was led to the welding head by means of an optical fiber with a diameter of 600 μm , air flow 15 L/min. The optical system consists of collimating lens with a focal length of 200 mm and focusing lens with focal length 200 mm.



Fig. 1. Fusion lines obtained on ADI with laser beam welding without preheating

A systematic research of the window power (P) - welding speed (W_s) was carried out by making fusion lines on cast iron plates without preheating, in order to determine some domains of weldability (fully penetrated weld seam, having a correct geometry for allow further characterization). A crack can be noticed in Figure 1.

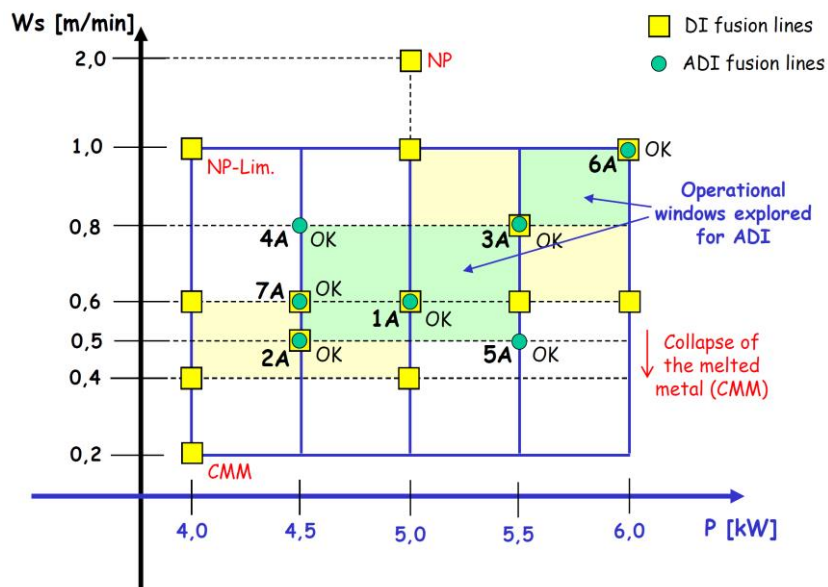


Fig. 2. Operational windows of parameters (P = power, W_s = welding speed) used for achieving of fusion lines on ADI plates (o) compared with DI plates (□) [12] (NP-Lim = non-penetration limit; NP = non-penetration; P-Lim = allowable penetration limit; OK = complete penetration)

Seven fusion lines were performing on the ADI plates: 5 fusion lines with parameters (P , Ws) that provided the best fusion lines on the DI cast iron plates [12] and two other fusion lines (4A and 5A) with different values (P , Ws), to delimit an optimal weldability range for ADI (Figure 2).

On first examination of the obtained results it can be concluded that from the point of view of the geometry of the fusion lines, there are no significant differences (in the parametric range P , V explored) between DI [12] and ADI. Unsatisfactory domains were characterized by: collapse of the metal bath, incomplete penetration, quality of fusion lines (geometry, compactness).

During this study, several parameters were tested to identify their influence on the geometry, compactness of the welding seams or even on the mechanical behaviour. These tests allow us to define the influence of laser power and welding speed.

3. Results and Discussions

The metallographic analysis aims to highlight the main metallographic constituents of the fusion lines specific to each area: the base material, the heat affected zone and the material melted by the laser beam and subsequently solidified. Tests were performed by optical microscopy using a metallographic microscope LEICA, WILD M420 (from Laser and Materials Treatments laboratory, Le Creusot). Representative samples were cut perpendicular to the fusion lines. After the sample preparation steps the reagent used was Nital 3%. The cutting of the specimens was done with BUEHLER cutting machine, model ABRASIMET 2, using abrasive disc and water jet in order to cool the area subjected to thermal stress.

The results of the application of laser welding regimes are highlighted in optical microscopy of the fusion line and heat affected zone. The microstructures magnification of the fusion line was 10x and of the heat affected zone (HAZ) and melted zone (MZ) was 500x.

The microstructure of the base material contains nodular graphite, acicular ferrite and retained austenite (Figures 3...9b).

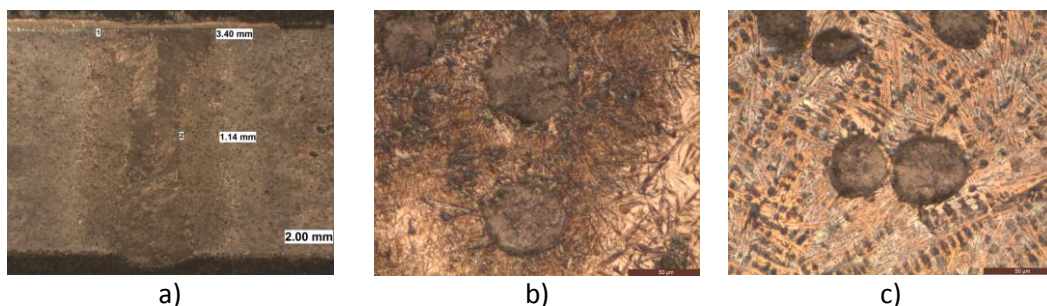


Fig. 3. *Optical microscopy, ADI samples, $P = 4.5$ [kW] and $Ws = 0.8$ [m/min]: (a) microstructure of fusion line, (b) microstructure of the HAZ, (c) microstructure of the MZ*

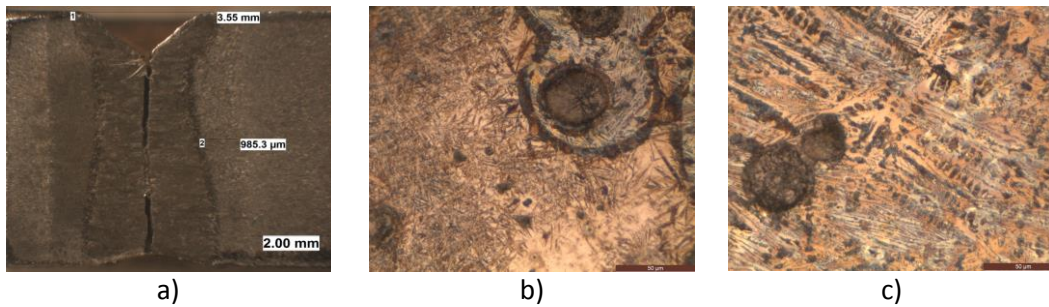


Fig. 4. *Optical microscopy, ADI samples, $P = 5.5$ [kW] and $W_s = 0.8$ [m/min]: (a) microstructure of fusion line, (b) microstructure of the HAZ, (c) microstructure of the MZ*

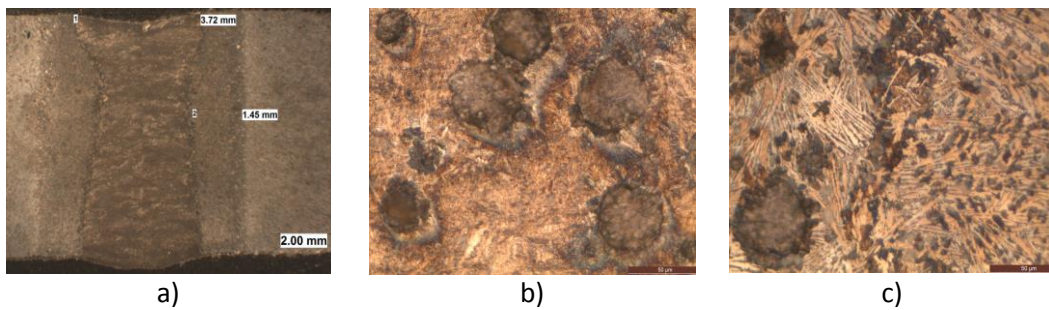


Fig. 5. *Optical microscopy, ADI samples, $P = 4.5$ [kW] and $W_s = 0.6$ [m/min]: (a) microstructure of fusion line, (b) microstructure of the HAZ, (c) microstructure of the MZ*

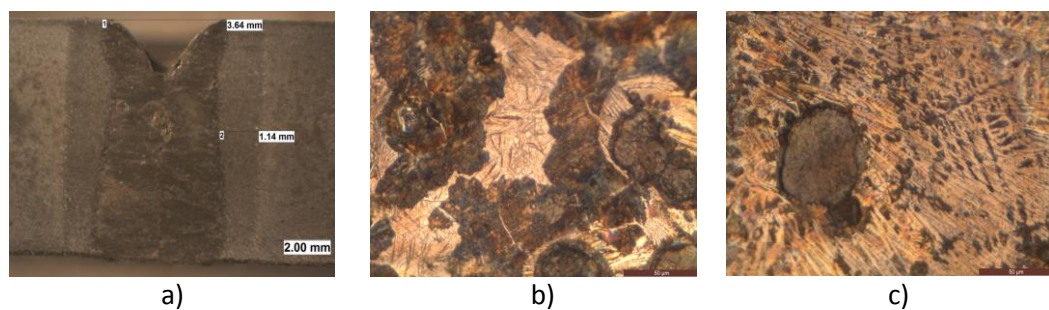


Fig. 6. *Optical microscopy, ADI samples, $P = 5$ [kW] and $W_s = 0.6$ [m/min]: (a) microstructure of fusion line, (b) microstructure of the HAZ, (c) microstructure of the MZ*

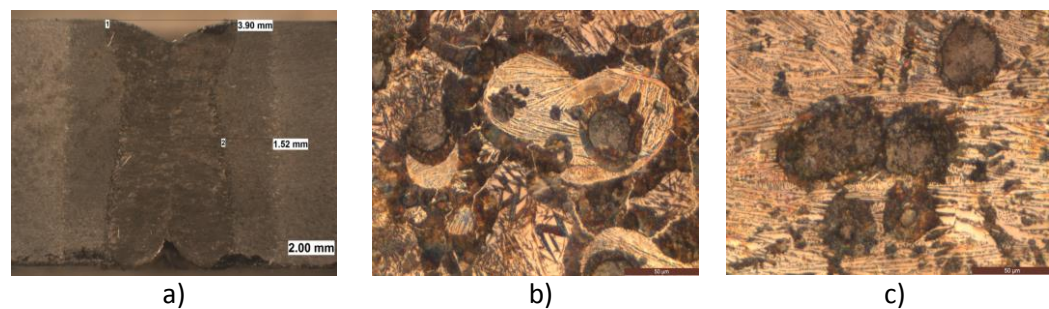


Fig. 7. *Optical microscopy, ADI samples, $P = 4.5$ [kW] and $W_s = 0.5$ [m/min]: (a) microstructure of fusion line, (b) microstructure of the HAZ, (c) microstructure of the MZ*

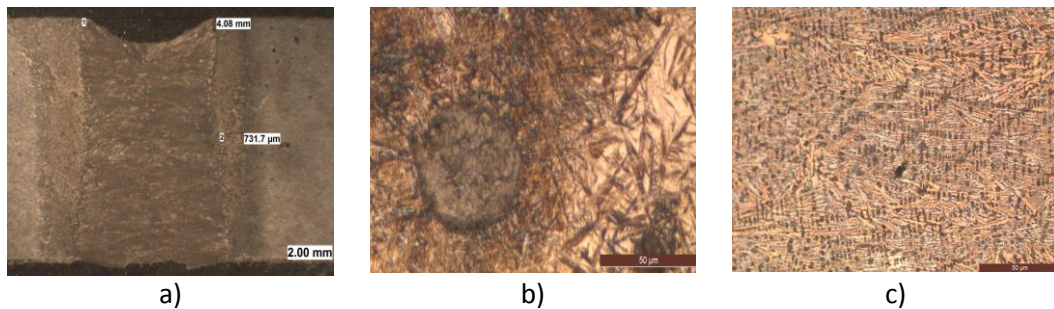


Fig. 8. *Optical microscopy, ADI samples, $P = 5.5$ [kW] and $W_s = 0.5$ [m/min]: (a) microstructure of fusion line, (b) microstructure of the HAZ, (c) microstructure of the MZ*

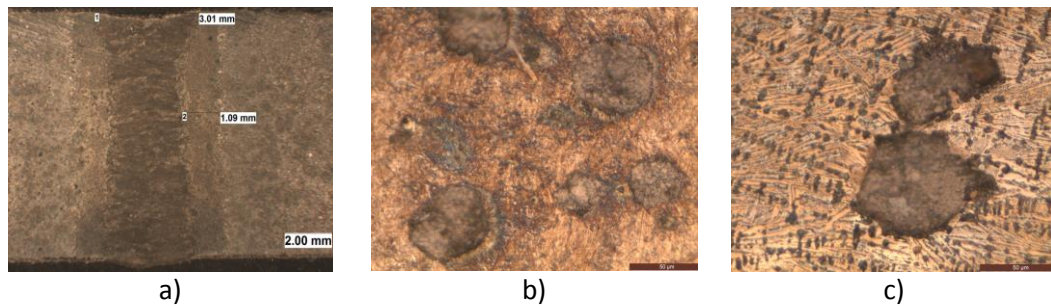


Fig. 9. *Optical microscopy, ADI samples, $P = 6$ [kW] and $W_s = 1$ [m/min]: (a) microstructure of fusion line, (b) microstructure of the HAZ, (c) microstructure of the MZ*

For each pair of tasted parameters (P - W_s) there were measured the melted zone (MZ) and heat affected zone (HAZ) thicknesses (Figure 10).

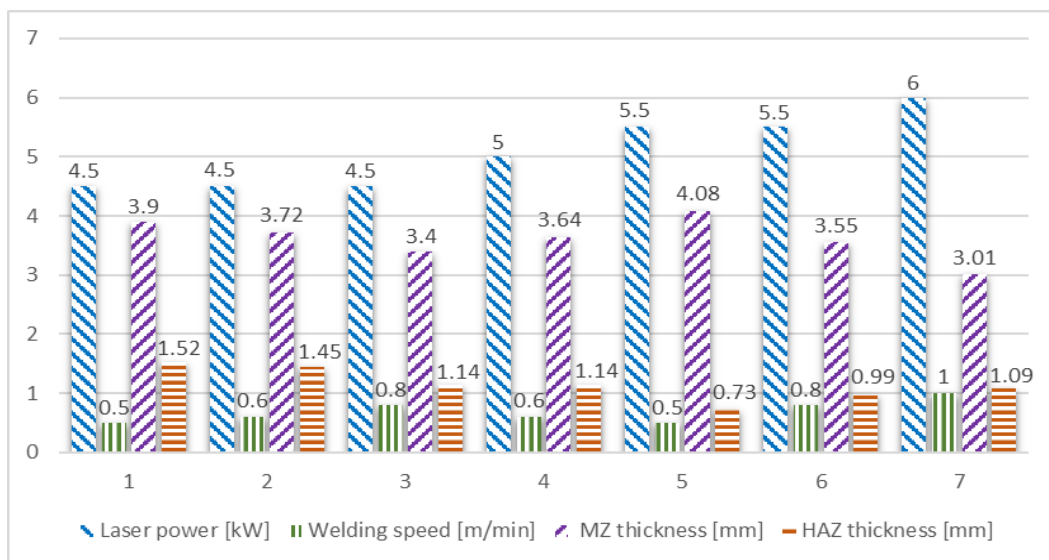


Fig. 10. *Variation of the thickness of the metal bath with the laser power and welding speed on ADI samples without preheating*

The fusion lines have the shape of a "keyhole". The microstructure of heat affected zone is composed of graphite, perlite and martensite, and in melted and solidified zone graphite, ferrite and cementite. Due to the high power ($P = 5...5.5$ kW) and the low welding speeds ($Ws = 0.5...0.8$ m/min) there is a collapse of the metal bath (Figures 4, 6, 8). In the case of using the power of 5.5 kW and the welding speed of 0.8 m/min, a dent in a V-shape of the metal bath is observed, the concentration of internal stresses at solidification producing a pronounced crack (Figure 4a), which led to the separation of the fusion line.

Compared to the fusion lines made on DI [12] without preheating, it is found that the melted zone has a similar thickness, but the width of the heat affected zone is larger, similar to the HAZ thickness of the fusion lines on preheated DI. As the welding speed increases, keeping the laser power constant, the thickness of the melted metal bath and HAZ decrease (Figure 10).

4. Conclusions

The research carried out in this paper allowed some main conclusions. Concerning the obtained fusion lines geometry, the results are acceptable. Regarding the microstructure, the heat affected zone is composed of graphite, perlite and martensite, and the melted and solidified zone contained graphite ferrite and cementite. It has been observed that by increasing the welding speed for the fusion lines, the penetration depth decreases. Thus, maintaining a constant laser power of 4.5 kW and increasing the welding speed in the range of 0.5-0.8 m/min, leads to a decrease of MZ thickness (from 3.9 to 3.4 mm) and of HAZ thickness (from 1.52 to 1.14 mm). On the other hand, maintaining a constant welding speed of 0.8 m/min and increasing the laser power, was found an increasing of the MZ thickness (from 3.4 to 3.55 mm) and a decreasing of HAZ thickness (from 1.14 to 0.99 mm). For better results on reducing or avoiding the cracks, it is indicated the preheating.

Acknowledgements

We would like to thank professor Adel Nofal from Central Metallurgical Research and Development Institute Egypt, for providing ADI materials. We also thank to professor Eugen Cicala and the staff of the research center from University of Bourgogne, Laboratoire Interdisciplinaire Carnot de Bourgogne (ICB) - Laser et Traitement des matériaux (LTm) for their support.

References

1. Agüera, F.R., Ansaldi, A., Reynoso, A., Fierro, V., Villar, N.A., Aquino, D., Ayllón, E.S.: *Análisis de soldadura de fundiciones ADI con electrodos de Fe-Ni*, CONAMET/SAM 2008.
2. Bejinariu, C., Munteanu, C., Florea, C.D., Istrate, B., Cimpoesu, N., Alexandru, A., Sandu, A.V.: *Electro-chemical Corrosion of a Cast Iron Protected with a Al_2O_3 Ceramic Layer*. In: *Revista de Chimie* **69** (2018) No. 12, p. 3586-3589.

3. Bendaoud, I., Mattei, S., Cicala, E., Tomashchuk, I., Andrzejewski, H., Sallamand, P., Mathieu, A., Bouchaud, F.: *The Numerical Simulation of Heat Transfers During A Hybrid Laser- MIG Welding Using Equivalent Heat Source Approach*. In: Optics & Laser Technology **56** (2014), p. 334-342.
4. Cicala, E., Duffet, G., Grevey, D.: *Optimization of the Laser Welding of Aluminium Alloys Used In Aeronautics*. In: Nonconventional Technologies Review **1** (2008), p. 9-16.
5. Guesser, W.L., Lopes, C.L., Bernardini, P.A.N.: *Austempered Ductile Iron with Dual Microstructures: Effect of Initial Microstructure on the Austenitizing Process*. In: Inter Metalcast (2020), <https://doi.org/10.1007/s40962-019-00397-y>.
6. Harding, R.A.: *The Production, Properties and Automotive Applications of Austempered Ductile Iron*. In: Kovove Mater. **45** (2007), p. 1-16.
7. Hayrynen, K.L., Keough, J.R.: *Austempered Ductile Iron - The State of the Industry in 2003*, 2003 Keith D. Millis Symposium.
8. Ignat, S., Sallamand, P., Nichici, A., Vannes, A.B., Grevey, D., Cicala, E.: *MoSi₂ Laser Cladding - A Comparison Between Two Experimental Procedures: Mo-Si Online Combination and Direct Use of MoSi₂*. In: Optics & Laser Technology **33** (2001), p. 461-469.
9. Labbe, E., Serban, F., Nicoara, M., Lodini, A.: *Evaluation of the Residual Stresses and Determination of the Proportion of Residual Austenite in an Austempered Ductile Iron Having Undergone Thermo Mechanical Treatments*. In: Materials Science Forum 571-572 (March 2008), p. 95-100.
10. Mesko, J., Hopko, A., Fabian, P.: *Repairing Technology of High-Strength Cast Irons*. In: Special Issue 2, Volume VI, May 2011, p. 106-111.
11. Mon, I.C., Tierean, M.H.: *A Review on Tests of Austempered Ductile Iron Welding*. In: Bulletin of the Transilvania University of Braşov, (2015) Vol. 8 (57), Series I, p. 59-66.
12. Mon, I.C., Tierean, M.H., Cicala, E., Pilloz, M., Tomashchuk, I., Sallamand, P.: *Characterization of Fusion Lines Obtained with Laser Welding On Ductile Iron Plates*. In: Solid State Phenomena **254** (2016), p. 33-42.
13. Mon, I.C., Tierean, M.H., Nofal, A.: *Research on GTAW/SMAW Weldability of ADI/DI using Electrodes ENi-CI and ENiFe-CI-A*. In: Advanced Materials Research **1128** (2015), Trans Tech Publications, Switzerland, p. 242-253.
14. Mon, I.C.: *Cercetări privind sudabilitatea fontelor ADI (Researches Concerning the Weldability of Austempered Ductile Iron)*. In: Ph.D. Thesis, Transilvania University of Braşov, Braşov, Romania, 2017.
15. Nofal, A., Amin, M., Sayed, M.: *Weldability of ADI and the Applied NDT Methods*. In: South African Metal Casting Conference 2017, www.metalcastingconference.co.za.
16. Riposan, I., Sofroni, L., Chişamera, M.: *Fonta bainitică (Bainite Cast Iron)*. Editura Tehnică, Bucureşti, 1988.
17. ASTM A897 / A897M-03, *Standard Specification for Austempered Ductile Iron Castings*, ASTM International, West Conshohocken, PA, 2003, www.astm.org.